

This document was prepared in conjunction with work accomplished under Contract No. AT(07-2)-1 with the U.S. Department of Energy.

## DISCLAIMER

This report was prepared as an account of work sponsored by an agency of the United States Government. Neither the United States Government nor any agency thereof, nor any of their employees, makes any warranty, express or implied, or assumes any legal liability or responsibility for the accuracy, completeness, or usefulness of any information, apparatus, product or process disclosed, or represents that its use would not infringe privately owned rights. Reference herein to any specific commercial product, process or service by trade name, trademark, manufacturer, or otherwise does not necessarily constitute or imply its endorsement, recommendation, or favoring by the United States Government or any agency thereof. The views and opinions of authors expressed herein do not necessarily state or reflect those of the United States Government or any agency thereof.

This report has been reproduced directly from the best available copy.

Available for sale to the public, in paper, from: U.S. Department of Commerce, National Technical Information Service, 5285 Port Royal Road, Springfield, VA 22161

phone: (800) 553-6847

fax: (703) 605-6900

email: [orders@ntis.fedworld.gov](mailto:orders@ntis.fedworld.gov)

online ordering: <http://www.ntis.gov/support/index.html>

Available electronically at <http://www.osti.gov/bridge>

Available for a processing fee to U.S. Department of Energy and its contractors, in paper, from: U.S. Department of Energy, Office of Scientific and Technical Information, P.O. Box 62, Oak Ridge, TN 37831-0062

phone: (865)576-8401

fax: (865)576-5728

email: [reports@adonis.osti.gov](mailto:reports@adonis.osti.gov)

CC: J. W. Croach-  
A. A. Johnson, Wilm.  
T. C. Evans, SRP  
C. H. Ice-  
L. H. Meyer, SRL  
G. Dessauer  
B. C. Rusche  
S. Mirshak  
P. L. Roggenkamp-  
E. J. Hennelly  
E. L. Albenesius-  
W. C. Reinig  
P. H. Permar  
W. R. McDonell  
E. F. Sturcken  
A. R. Boulogne  
P. K. Smith  
C. W. Krapp  
C. L. Angerman  
TIS File Copy

TIS FILE  
RECORD COPY

Vital Records Copy

MEMORANDUM

October 4, 1974

TO: R. T. HUNTOON

FROM: <sup>THG</sup> T. H. GOULD, JR.

RADIATION DAMAGE BY  $^{252}\text{Cf}$  FISSION FRAGMENTS

INTRODUCTION

Recently W. R. McDonell suggested using  $^{252}\text{Cf}$  fission fragments to simulate fast neutron displacement damage in reactor materials. (1) Accelerator-generated heavy ions are used currently in radiation effect experiments for the Fast Breeder Reactor (FBR) and Controlled Thermonuclear Reactor (CTR) programs. (2) Such experiments are primarily concerned with observing by transmission electron microscopy (TEM) the voids formed from vacancies created by heavy ion displacements in metals and alloys. Nucleation of these voids is assisted by helium atoms which are generated by  $(n,\alpha)$  reactions in fission reactors or are injected directly from the plasma in a CTR. Helium from  $^{252}\text{Cf}$   $\alpha$ -radiation would be concurrently injected with fission fragments into materials placed in contact with a  $^{252}\text{Cf}$  source. If adequate displacement rates could be achieved, such sources could provide a more effective means to study the influence of He atoms on voids than accelerator bombardment, which requires helium preinjection.

This report discusses the feasibility of using  $^{252}\text{Cf}$  in the form of Cf-oxide as a radiation damage source. Theoretical estimates of displaced-atom densities and helium atom concentrations in aluminum and iron are reported.

## SUMMARY

The relatively low displacement rates achievable with  $^{252}\text{Cf}$  (compared with accelerator experiments) may limit its usefulness as a radiation damage source. Fission fragments are generated by  $^{252}\text{Cf}$  at a rate of  $1.23 \times 10^{12}/\text{g}\cdot\text{sec}$ , or about  $2.4 \times 10^{12}/\text{cm}^3\cdot\text{sec}$  from a strong  $\text{Cf}_2\text{O}_3$  source ( $\approx 6 \text{ mg } ^{252}\text{Cf}$ ). The induced displacement damage in an adjacent aluminum or iron target will be about  $10^{-6}$  displacements per atom per second (dpa/s) at the surface, decreasing monotonically to zero at the maximum range of the fission fragments. This displacement rate is slightly lower than that predicted for a FBR or CTR and several orders of magnitude less than accelerator-produced damage, but is about ten times the damage rates presently available in SRP thermal reactors.

In addition to fission fragment-induced displacement damage, helium atoms from  $^{252}\text{Cf}$   $\alpha$ -decay will be deposited in a surface layer of exposed metal at maximum relative concentrations of about 225 ppm/dpa (iron) to 350 ppm/dpa (aluminum). These relative exposures are some 12 to 20 times exposures anticipated in CTR's and two to three orders of magnitude greater than fission reactors.

## CONCLUSIONS

Metals or alloys exposed to fast neutrons or ions exhibit detectable voids at damage doses in the range of 0.1 to  $\approx 10$  dpa.<sup>(3)</sup> The extent of void formation and growth is highly dependent upon certain physical properties (melting, temperature, dislocation density, impurities, etc) of the metal or alloy. For example, pure aluminum exhibits detectable voids at exposures of 0.1 dpa,<sup>(3)</sup> while no voids have been detected in 6063 Al at exposures of about 10 dpa.<sup>(4)</sup> Neglecting the effect of injected helium, about 120 days exposure to the proposed  $^{252}\text{Cf}$  source would be required to produce 10 dpa in aluminum or iron. Just a few hours exposure to accelerator-produced heavy ions could accomplish the same effect. Thus, judged solely on displaced-atom production,  $^{252}\text{Cf}$  is not a very practical radiation damage source.

The one possible advantage of  $^{252}\text{Cf}$  sources over accelerators is the simultaneous implantation of helium atoms with fission fragment-induced displacements in an adjacent target. Preliminary results indicate that helium concentrations between 0.1 and 150 atomic ppm will be important for fuel cladding and structural material damage studies in FTR's.<sup>(5)</sup> In CTR studies, concentrations of 300 ppm or greater will be required.<sup>(6)</sup> Presently there is no convenient mechanism for injecting helium concurrently with displacement damage.  $^{252}\text{Cf}$  sources could be used for this purpose, at least to study the effects of very large helium atom densities. Helium concentrations of 300 ppm can be achieved in about 10 days using a strong Cf-oxide source. The concurrent displaced-atom density will be only about one dpa, or some 20 times lower than expected in CTR blankets receiving

comparable helium exposures. The difference is even much greater for FTR's and thermal fission reactors.

For the above reasons, Cf-oxide sources would be limited to studying upper limit effects of helium in damaged metals and alloys. Such studies would be more applicable to CTR's than fission reactors. Aluminum would be a good initial candidate to study these effects because of its sensitivity to void formation at reasonable doses and low temperatures. Other candidate metals would include magnesium, because of its sensitivity to cavity formation, and iron (stainless steel), because of its potential use in structural alloys for CTR's.

## DISCUSSION

The transuranium isotope  $^{252}\text{Cf}$  decays through two processes: spontaneous fission ( $t_{1/2} = 85.5 \text{ y}$ ) and alpha emission ( $t_{1/2} = 2.65 \text{ y}$ ).<sup>(7)</sup> Of the  $1.23 \times 10^{12}$  fission fragments produced per gram per second, half (light group) are emitted with an average kinetic energy (E) of 104.1 Mev and average atomic number (Z) of 42 and mass (A) of 106.4. The other half (heavy group) have average values of 79.25 Mev, 55 and 141.7 for E, Z, and A, respectively. These highly energetic and massive particles lose energy in solids through elastic collisions with electrons (ionization) and through interactions with atoms as a whole (nuclear displacements). The latter are responsible for the production of observable damage phenomena, such as dislocations and voids. Alpha particles emitted by  $^{252}\text{Cf}$  also cause some displaced-atom production, while the implanted helium may affect the formation of voids or cavities in the target. Calculations to determine the displaced-atom density and helium atom concentration as a function of penetration in aluminum and iron, as well as the target's radioactivity caused by the implanted fission products, are discussed in the following sections.

### Displaced Atom Density

The density of displaced atoms generated by the passage of energetic fission fragments through a solid was calculated by modifying the model used by Kulcinski et al.<sup>(8)</sup> to predict displacement densities from accelerator-generated heavy ions. This model combines the Lindhard (or LSS) energy loss theory<sup>(9)</sup> with a Kinchin and Pease (KP)<sup>(10)</sup> displacement approximation. As briefly outlined in Appendix A, the procedure involves:

- Calculating the average ranges of the mean light and heavy fragments as a function of energy (LSS)
- Calculating the rates of energy loss in nuclear collisions as a function of penetration into the solid (LSS)
- Converting the rates of nuclear energy loss into displaced-atom densities (KP).

The resulting displacement density function, which applies strictly to monoenergetic and unidirectional ions, can be written as

$$N(x) = \frac{\omega S_n(x) \phi}{2 E_d} \quad (1)$$

where  $N(x)$  is the number of atoms displaced per cc at a penetration  $x$  into the target,  $\phi$  is the particle flux, and  $E_d$  is the displacement energy ( $\approx 25$  ev).  $S_n(x)$  above represents the rate of energy transfer in primary nuclear collisions (the energy transferred by the bombarding ions to the lattice atoms, not electrons, in ev/cm). The displacement efficiency,  $\omega$  ( $< 1$ ), represents the fraction of this energy which goes into secondary and lower order nuclear collisions. The energy transfer function,  $S_n(x)$ , was calculated for the mean light (MLF) and mean heavy (MHF) fission fragments of  $^{252}\text{Cf}$  in aluminum and iron (Appendix A). Energy loss rates (electronic and nuclear) for the MHF fragment in aluminum are shown in Figure 1.

Equation 1, as mentioned above, applies to a monoenergetic beam of heavy ions. In the case of a  $^{252}\text{Cf}$  fission fragment source, the heavy ions would originate in a volume of finite thickness adjacent to the target so that both directional and self-absorption effects have to be considered. Only fission fragments generated within a source thickness equal to their maximum range will reach the target and produce damage. The exact solution to this problem would involve the product  $\phi(x, E) \cdot \left(\frac{dE}{dx}\right)_n$ , where  $\phi(x, E)$  is the flux density of fission

fragments at the penetration  $x$  having energy  $E$ , and  $\left(\frac{dE}{dx}\right)_n$  is the nuclear stopping power. Since calculation of  $\phi(x, E)$  is beyond the scope of the present study, two approximations have been made to simplify the problem (see Appendix B for details). First, the ranges (or rate of energy loss) of fission fragments in the  $\text{Cf}_2\text{O}_3$  source are assumed equal to those in the target material. Second, the nuclear energy transfer function,  $S_n(x)$  of Figure 1, has been replaced by a Gaussian distribution about the mean range,  $R$ , of the fission fragment group,

$$S_n(r) \approx \frac{E_T}{\alpha \sqrt{\pi}} \exp\left[-\frac{(r-R)^2}{\alpha^2}\right] \quad (2)$$

In Equation 2,  $E_T$  is the total energy lost in primary nuclear collisions (total energy under  $S_n(x)$ ),  $r$  is the distance traveled by the fragment from its origin in the source, and  $\alpha$  is the range straggling parameter for either the mean light or mean heavy fission fragment. In addition to these approximations, the source thickness is assumed to be greater than the maximum range of fission fragments.

Applying the above assumptions to Equation 1, Appendix B shows that the displaced-atom density (dpa/s) as a function of penetration  $x$

into the target (normal to surface) can be approximated by

$$D(x) \approx \frac{n_f \omega E_T}{4E_d N} (1 - x/R)^3; \quad x \approx R - 2\alpha \quad (3)$$

where  $n_f$  is the number of light or heavy fission fragments generated in the source (f.f./cm<sup>3</sup>·sec) and  $N$  is the target atom density (atoms/cm<sup>3</sup>). The product  $\omega E_T$  represents the energy transferred in nuclear collisions;  $\omega E_T/2E_d$  represents the total number of displacements per fission fragment. Values for  $\omega$ ,  $E_T$ , and  $R$  used to calculate the damage function,  $D(x)$ , in aluminum and iron are listed in Table I. The straggling parameter  $\alpha$  is of the order of 1/10 the range so that Equation 3 applies to about 80% of the total penetration (see Appendix A).

For a Cf<sub>2</sub>O<sub>3</sub> source with a density of 10 g/cc containing 20% <sup>252</sup>Cf<sub>2</sub>O<sub>3</sub>,  $n_f$  is  $\approx 1.2 \times 10^{12}$  f.f./cm<sup>3</sup> sec. About 6 mg of oxide (540 mCi) would be required for a 0.3 cm<sup>2</sup> target foil. Substituting the values from Table I into Equation 3, the displaced-atom density at the surface of an aluminum target will be about  $9 \times 10^{-7}$  dpa/sec ( $1 \times 10^{-6}$  dpa/sec for iron). The relative and combined displaced-atom densities from the MLF and MHF groups as a function of penetration into an aluminum target are shown in Figure 2. Damage decreases about 50% at a penetration of seven microns, or about 40% of the maximum range.

Figure 3 compares typical displacement rates currently attainable from reactors, charged particle accelerators, and a <sup>252</sup>Cf fission fragment source. Damage rates from <sup>252</sup>Cf are at least an order of magnitude greater than those produced in present SRP cores, but are slightly lower than predicted for fast reactors and CTR's, and several orders of magnitude lower than typical accelerator induced rates.<sup>(8)</sup> Fission fragments from <sup>235</sup>U in highly enriched uranium would be required in thermal reactors to achieve displacement rates comparable to accelerators. Considering an iron target in contact with a 90% enriched UO<sub>2</sub> fission fragment source in a thermal flux of  $\approx 10^{14}$  n/cm<sup>2</sup> sec, the surface displacement rate will be  $\approx 1 \times 10^{-3}$  dpa/sec, or some three orders of magnitude greater than that caused by a <sup>252</sup>Cf source.

### Helium Atom Injection

The generation rate of 6 Mev  $\alpha$ -particles from the 6 mg Cf<sub>2</sub>O<sub>3</sub> source considered above will initially be about  $3.6 \times 10^{13}$  particles/cm<sup>3</sup> sec. This rate is half-life dependent, varying with time  $t$  as  $3.6 \times 10^{13} x [1 - \exp(-\lambda t)]$ . Since  $\lambda = 7.16(10)^{-4}$  d<sup>-1</sup>, the He atom generation rate remains fairly constant over 200 days irradiation.

The distribution of helium atoms in the target can be calculated in a manner similar to that described in Appendix B. The number density of He atoms is approximated by

$$N(x) \approx \int_{\text{Source Volume}} \frac{S_v}{4\pi r^2} \frac{1}{\alpha\sqrt{\pi}} \exp\left[-\frac{(r-R)^2}{\alpha^2}\right] dV \quad (4)$$

where  $S_v$  is the source generation rate (He atoms/cm<sup>3</sup> sec). Integrating as in Appendix B, Equation 4 reduces to

$$N(x) \approx \frac{S_v}{2} \left(1 - x/R\right) \quad ; \quad x < R - 2\alpha \quad (5)$$

This equation applies to over 98% of the  $\alpha$ -particles' range since the range straggling parameter  $\alpha$  is about 0.01R.<sup>(11)</sup> The range of alpha particles in aluminum was determined from range data for protons<sup>(11)</sup> using the relation

$$R_\alpha(E) = R_p \left( \frac{M_p \cdot E}{M_\alpha} \right)$$

For 6 Mev alpha particles, the calculated range is about 30 microns, or about twice the range of <sup>252</sup>Cf fission fragments. The ratio of He atom concentration to displaced-atom density from fission fragments is shown by the dashed curve in Figure 2. In aluminum, this ratio will be about 350 atomic ppm He/dpa at the target surface, increasing with penetration due to the greater range of the  $\alpha$  particles. In iron the relative concentration will be about 225 ppm He/dpa at the surface. These relative concentrations are 12 to 20 times greater than expected in CTR's<sup>(6)</sup> and some two to three orders of magnitude greater than obtained in fission reactors.<sup>(3,5)</sup> Helium concentrations from a <sup>252</sup>Cf source having a thickness between the ranges of alpha particles and fission fragments will be lower than the values calculated above.

The displacement damage induced in a metal target by the 6 Mev alpha particles of <sup>252</sup>Cf was also considered. Because of their smaller mass and correspondingly high velocities, displacement collisions of 6 Mev alphas with Al or Fe target atoms are of the Rutherford type<sup>(12)</sup> so that the LSS theory of Appendix A does not apply. Instead, a model derived by Kinchin and Pease for energy loss in whole atom Rutherford collisions was used.<sup>(10)</sup> In aluminum about 300 displacements occur per 6 Mev alpha particle. Assuming a damage distribution similar to Equation 3, the displaced-atom density at the target's surface from alpha particles will be about  $9 \times 10^{-8}$  dpa/sec, or about 10% of the number produced by fission fragments. At a penetration of seven microns, where the displaced-atom density from fission fragments is half its surface value, the relative alpha particle contribution will be about 15%.

### Induced Radioactivity

The major source of radioactivity induced in the target by exposure to <sup>252</sup>Cf radiation will be from the  $\beta$  and  $\gamma$  decay of implanted fission products. Contamination from implantation of <sup>252</sup>Cf on the target's

surface can be effectively removed prior to preparation of the target for TEM studies. Radioactivity caused by activation of target atoms by  $^{252}\text{Cf}$  neutrons is neglected.

To approximate the fission product induced activities, the empirical relationship developed by Way and Wigner for  $^{235}\text{U}$  fission product decay was used.<sup>(13)</sup> Emission of  $\gamma$  protons or  $\beta$  particles (#/sec) at time  $t$  (days) after the start of bombardment can be approximated as

$$R(t, T_0) \simeq 5 \times 10^{-6} S \cdot C \left[ (t - T_0)^{-0.2} - t^{-0.2} \right] \quad (6)$$

In this expression,  $S$  is the number of fission fragments injected into the target per day,  $T_0$  is the irradiation time in days, and  $C$  is a constant equal to 1.9 for  $\gamma$ -emission and 3.8 for  $\beta$ -emission. For a target with a  $0.3 \text{ cm}^2$  surface area exposed to the 6 mg  $\text{Cf}_2\text{O}_3$  source,  $S$  will be equivalent to about  $2.3 \times 10^{13}$  fissions/day. Assuming an exposure of 30 days (total displacement density of  $\approx 2.6 \text{ dpa}$ ) followed by one day of decay, Equation 5 gives a gamma activity of about 3 mCi. Taking 0.7 Mev as the average energy of the gamma protons,<sup>(7)</sup> the dose rate at one meter will be less than 2 mr/hr. Therefore, the exposed targets should present no serious handling problem.

THG:ehj

REFERENCES

1. W. R. McDonell, Memorandum to R. T. Huntoon, February 19, 1974.
2. D. I. R. Norris, "Voids in Irradiated Metals" (Parts I and II), Radiation Effects, 14 and 15, 1972.
3. J. O. Steigler, "Void Formation in Neutron-Irradiated Metals," Radiation-Induced Voids in Metals, CONF-710601, June, 1971.
4. E. F. Sturcken, C. W. Krapp, and G. B. Alewine, "Effects of Irradiation on 6063 Aluminum Structural Components in Savannah River Reactors," Nuclear Metallurgy, 19, August, 1973.
5. W. N. McElroy and H. Farrar, "Helium Production in Stainless Steel and Its Constituents as Related to LMFBR Development Programs," CONF-710601, June, 1971.
6. G. L. Kulcinski, R. G. Brown, R. G. Lott, and P. A. Sanger, "Radiation Damage Limitations in the Design of the Wisconsin Tokamak Fusion Reactor," Nucl. Technology, 22, April, 1974.
7. D. H. Stoddard, "Radiation Properties of Californium-252," DP-986, June 1965.
8. G. L. Kulcinski, J. J. Laidler, and D. G. Doran, "Simulation of High Fluence Fast Neutron Damage with Heavy Ion Bombardment," Radiation Effects, I, 195 (1971).
9. J. Lindhard, M. Scharff and H. E. Schiott, "Range Concepts and Heavy Ion Ranges (Notes on Atomic Collisions, II)," Mat. Fys. Medd. Dan. Vid. Selsk., 33, No. 14, 1963.
10. G. H. Kinchin and R. S. Pease, "The Displacement of Atoms in Solids by Radiation," Reports on Progress in Physics, 18, 1, 1955.
11. S. V. Starodubtsev and A. M. Romanov, The Passage of Charged Particles Through Matter, AEC-tr-6468, Chapt. 1, 1965.
12. B. T. Kelly, Irradiation Damage to Solids, Pergamon Press, N. Y. (1966), Chapt. 1.
13. S. Glasstone and A. Sesonski, Nuclear Reactor Engineering, D. Van Nostrand Co., N. Y., 1955, Chapt. 2.
14. H. W. Schmitt and F. Pleasonton, Nucl. Inst. and Meth., 40, 204, 1966.
15. J. Lindhard and P. V. Thomson, "Sharing of Energy Dissipation Between Electronic and Atomic Motion," Radiation Damage in Solids, Vol. 1, IAEA, Vienna (ST1/PUB/56), 1962.

TABLE I

PARAMETERS USED TO CALCULATE THE  
DISPLACED-ATOM DENSITIES IN Al AND Fe

<u>Parameter</u>	<u>Aluminum</u>		<u>Iron</u>	
	<u>MLF</u>	<u>MHF</u>	<u>MLF</u>	<u>MHF</u>
$E_T$ (Mev)	4.4	7.1	5.6	8.7
$\omega$	0.45	0.42	0.46	0.44
R (microns)	16	13	8.0	6.3
$\alpha/R$	0.08	0.11	0.08	0.11
$E_d$ (ev)	30	30	25	25

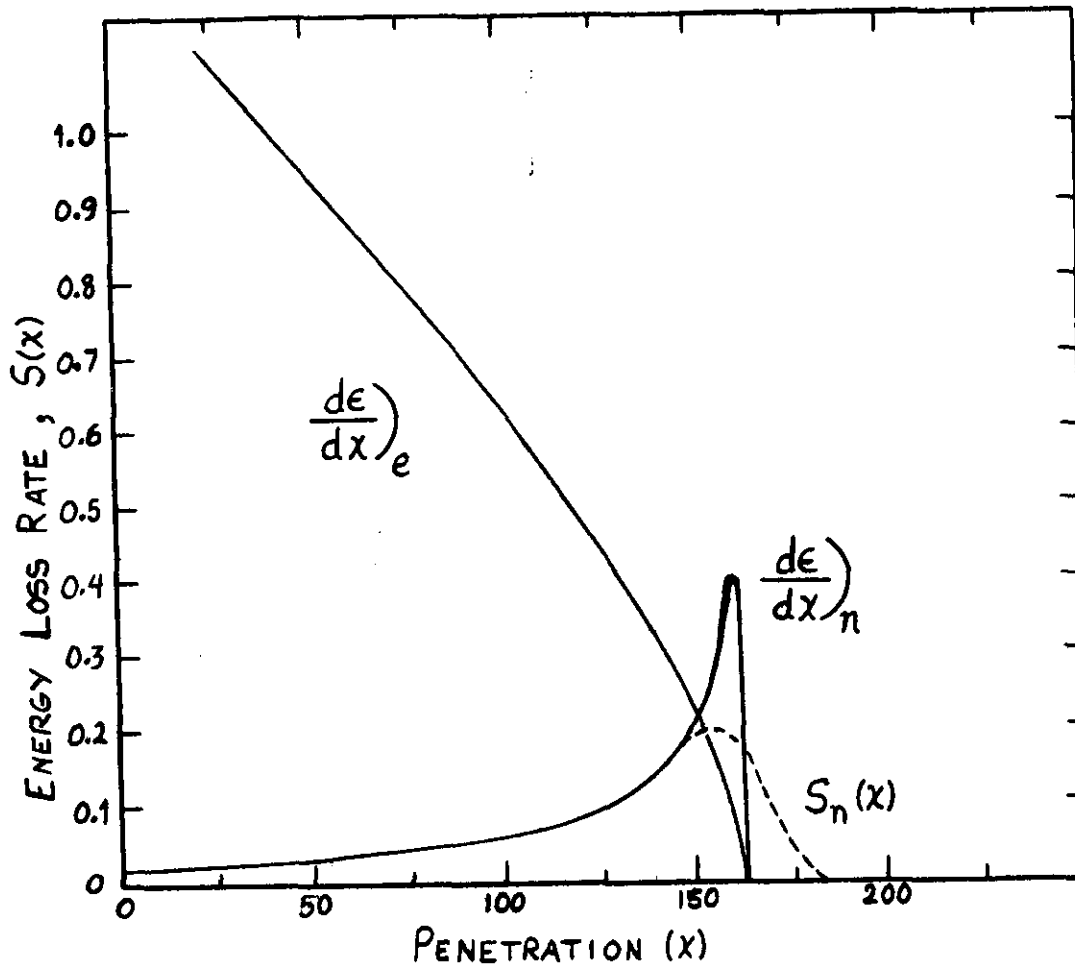


**FIGURE 1.** Energy loss rates,  $S(x)$  or  $d\epsilon/dx$ , for the mean heavy fission fragment in aluminum. Energy ( $\epsilon$ ) and penetration ( $x$ ) are defined in terms of LSS dimensionless parameters (see Appendix A). The subscript 'e' represents energy losses in electronic collisions, while 'n' represents losses in whole atom or nuclear collisions. The dashed curve,  $S_n(x)$ , represents the nuclear energy loss rate after straggling effects are accounted for.

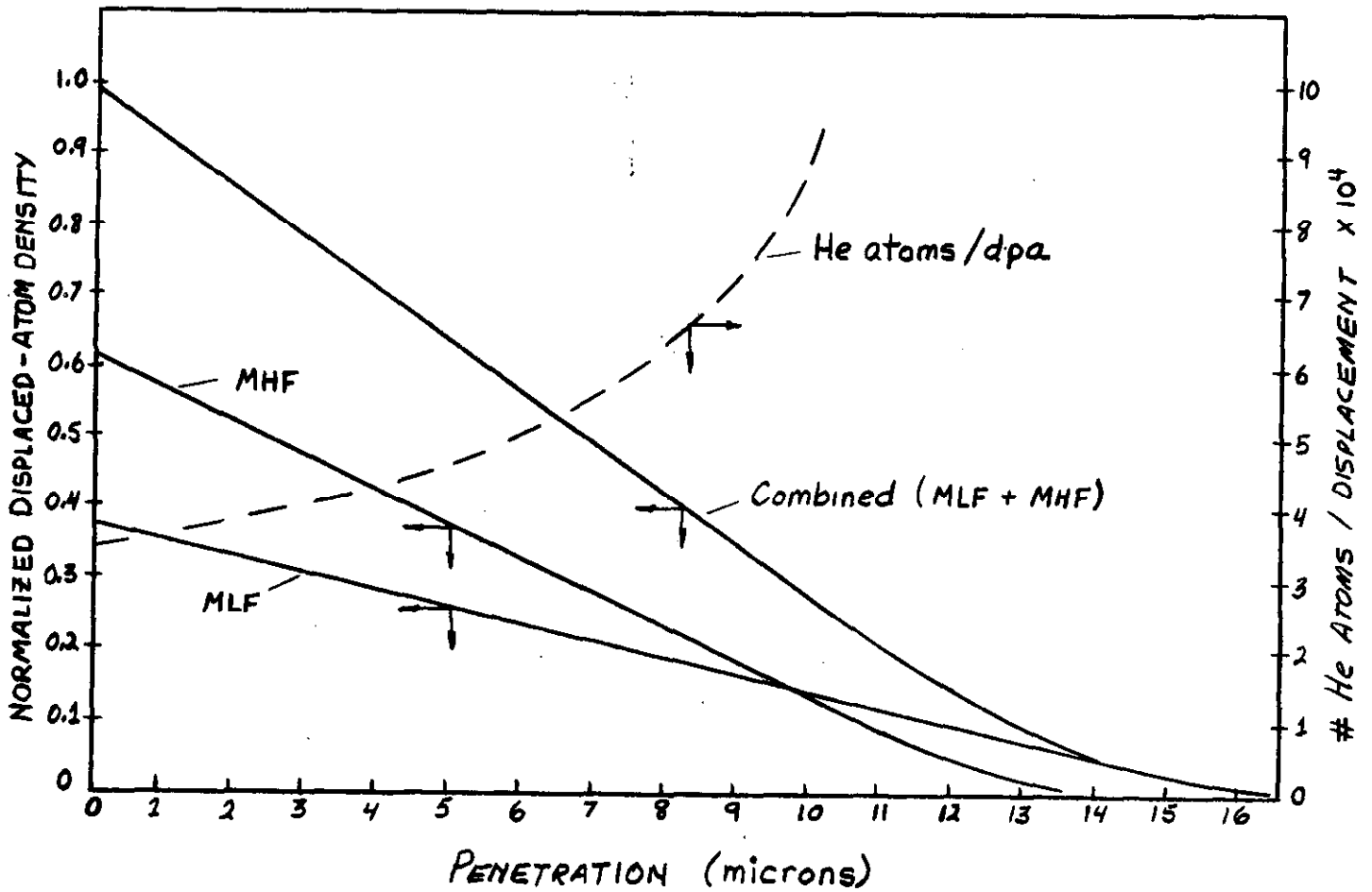


**FIGURE 2.** Normalized displaced-atom densities and relative helium atom concentration in aluminum. Dashed curve with positive slope represents the ratio of He atoms deposited to the number of fission-fragment induced displacements. Left ordinate values multiplied by  $9 \times 10^{-7}$  give displaced-atom density (displacement rate) in dpa/sec.

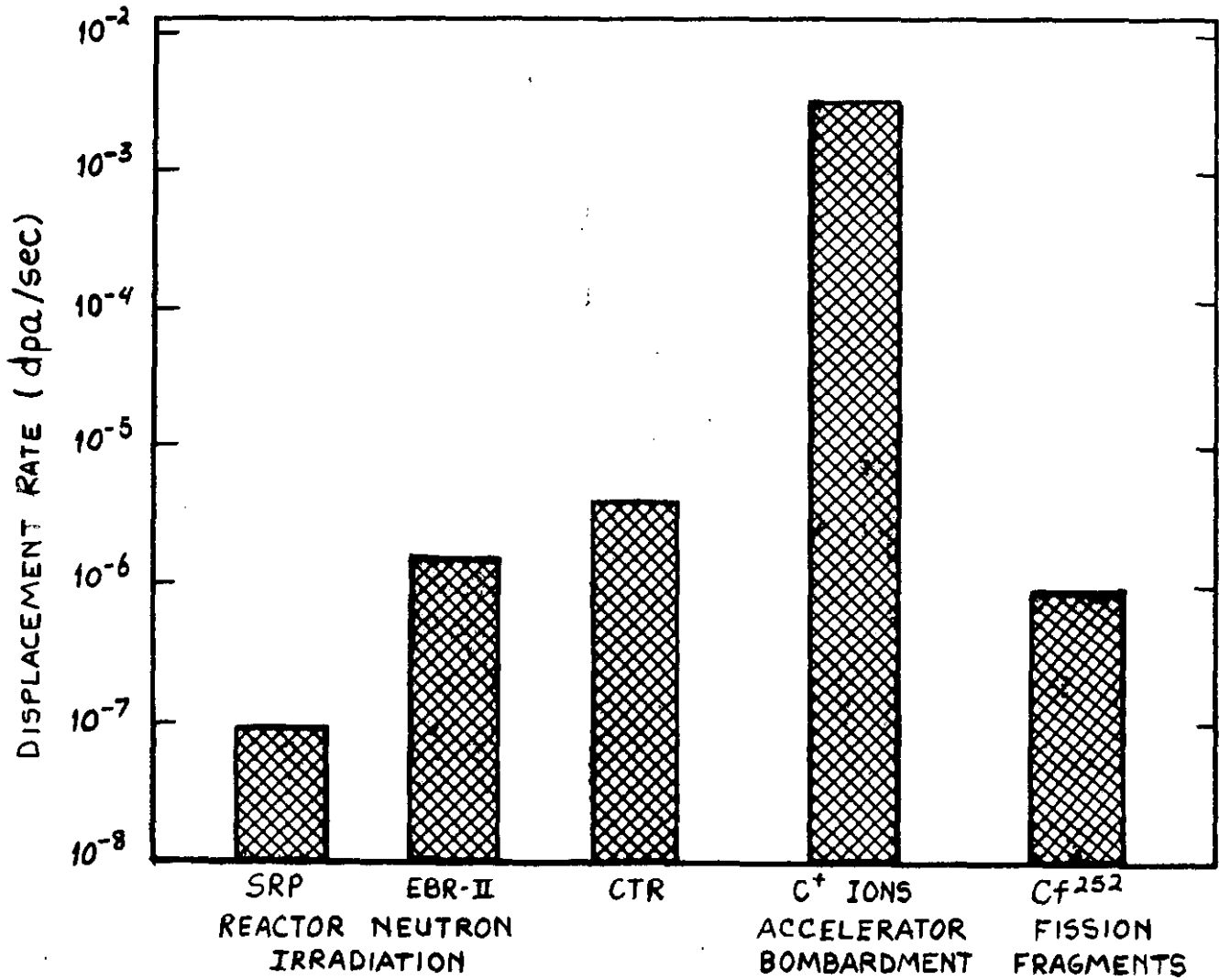


FIGURE 3. Displacement rates available from several damage sources.

APPENDIX ASUMMARY OF ENERGY LOSS CALCULATIONS

According to Kinchin and Pease, (10) the displaced atom density created by a heavy charged particle coming to rest in a solid is proportional to the energy transferred in nuclear collisions. To determine the nuclear energy loss or transfer rate with distance in a metal for the mean light (MLF) and mean heavy (MHF) fission fragments from  $^{252}\text{Cf}$ , it is first necessary to evaluate their nuclear and electronic stopping powers as well as their mean projected ranges. These quantities have been calculated using the Lindhard (LSS) theory. (9) This theory, based upon a Thomas-Fermi model of interacting atoms, considers energy losses by ionization and by nuclear collisions as uncorrelated and continuous processes. General features of the calculations based on LSS theory are briefly summarized below.

Energy Loss and Range Estimates

The energy  $E$  and range  $R$  in LSS theory are converted to dimensionless variables  $\epsilon$  and  $\rho$ , where

$$\epsilon = A \cdot E \text{ and } \rho = B \cdot R \quad \text{A.1)}$$

The constants  $A$  and  $B$  above are related to atomic properties (e.g., atomic number, mass, etc) of the incident particle and target atoms. Using the above notation, the nuclear stopping power,  $(d\epsilon/d\rho)_n$ , becomes a universal function of  $\epsilon$  and is independent of the incident particle and target atoms. Parametric curves for  $(d\epsilon/d\rho)_n$  have been presented by Lindhard, et al. (9) Similarly, the electronic stopping power can be approximated by  $(d\epsilon/d\rho)_e = k\epsilon^{1/2}$ , where  $k$  is also related to the atomic properties of the incident particle and target atoms.

Using this notation, the average range of either the MLF or MHF fragment is given by

$$\rho = \int \frac{d\epsilon}{(d\epsilon/d\rho)_e + (d\epsilon/d\rho)_n} \quad \text{A.2)}$$

The above equation represents the total path length of the incident fission fragment in the metal; however, the straight-line distance from the target's surface to the fragment's resting place is desired. This latter quantity,  $\bar{\rho}$ , is called the average projected range and is given in LSS theory by

$$\frac{\rho - \bar{\rho}}{\rho} = 4\psi(\epsilon, k) \quad \text{A.3)}$$

where  $\mu$  is the mass ratio of target and incident atoms and  $\psi(k, \epsilon)$  is a parametric function related to energy through  $\epsilon$  and to the atomic properties of incident and struck atoms through  $k$ . Parametric curves for both  $\rho$  and  $\psi$  are given by LSS(9) for several values of  $k$ . The projected ranges for both the MLF and MHF fragments as a function of energy in aluminum and iron were interpolated from the LSS curves.

Using this information, the energy loss rates,  $(d\epsilon/d\epsilon)_n$  and  $(d\epsilon/d\epsilon)_e$ , were converted from functions of energy to functions of penetration by noting that the distance traveled by the incident fragment in slowing down from initial energy  $\epsilon_m$  to energy  $\epsilon$  is given by

$$\chi(\epsilon) = \bar{\rho}(\epsilon_m) - \bar{\rho}(\epsilon) \quad \text{A.4}$$

The energy loss rate-range relationships,  $(d\epsilon/dx)_n$  and  $(d\epsilon/dx)_e$ , versus penetration, were determined for the MLF and MHF fragments in both aluminum and iron. The results for the MHF fragment in aluminum are shown in Figure 1.

### Straggling Effects

Statistical fluctuations in individual collisions cause the phenomenon known as range straggling. All ions of the same energy do not have the same range, but a distribution of ranges which can be approximated by the usual Gaussian form:

$$\frac{1}{n_0} \frac{dn}{dx} = \frac{1}{\alpha\sqrt{\pi}} \exp\left[-\frac{(r-\bar{\rho})^2}{\alpha^2}\right] \quad \text{A.5}$$

where  $\alpha$  is the range straggling parameter and  $\bar{\rho}$  is the mean projected range (in this form both are dimensionless). The above expression represents the number  $dn$  of incident particles having actual ranges between  $r$  and  $r+dr$ . Straggling parameters for the two fission fragment groups were determined from parametric curves (parameters are  $\epsilon$  and  $k$ ) given in Reference 9. In aluminum, the relative straggling ( $\alpha/R$ ) was about 3% for the MLF fragment and 4% for the MHF fragment.

The effect of range straggling on the rate of energy transfer in nuclear collisions is shown by the dashed curve in Figure 1.  $S_n(x)$ , which represents the total rate of nuclear energy transfer (ev/cm), was calculated from

$$S_n(x) \approx \int_0^{\infty} S(x-r) \frac{1}{\alpha\sqrt{\pi}} \exp\left[-\frac{(r-\bar{\rho})^2}{\alpha^2}\right] dr \quad \text{A.6}$$

where  $S_n(x-r)$  is the nuclear energy transfer rate evaluated at  $x$  for a particle with projected range  $r$ . The areas under the two curves,  $(d\epsilon/dx)_n$  and  $S_n(x)$ , are equivalent.

Since the above calculations pertain strictly to heavy monoenergetic ions having the properties of the MLF or MHF fragment of  $^{252}\text{Cf}$ , additional range dispersion or straggling associated with the energy and mass distributions of the two fission fragment groups had to be accounted for. For the purpose of this analysis, only energy dispersion was considered. The effective range straggling parameter for each fission fragment group was estimated from

$$\alpha^2 = \alpha_L^2 + \alpha_E^2 \quad \text{A.7)}$$

where  $\alpha_L$  represents range straggling from LSS theory and  $\alpha_E$ , the range dispersion associated with the group's energy distribution. The range dispersion parameter  $\alpha_E$ , which is the dominant term of Equation A.7, was determined from the experimental energy distribution of  $^{252}\text{Cf}$  fission fragments measured by Schmitt and Pleasonton.<sup>(14)</sup> Conversion from energy dispersion to range dispersion was made with the aid of energy-range relationships derived from LSS theory. Values of effective relative straggling for the MLF and MHF fragments are given in Table I.

### Displacement Efficiency

As indicated by Equation 1, only a fraction  $\omega$  of the energy transferred to target atoms by primary nuclear collisions will eventually go into secondary and lower order displacements (part of the primary knockon's energy may go into ionization events). Lindhard and Thomson<sup>(15)</sup> have calculated the total energy  $\nu(\omega E_T)$  of Eq. 3 dissipated in nuclear collisions by the MLF and MHF fragments of  $^{235}\text{U}$  in several elements. The displacement efficiency for the MLF and MHF fragments of  $^{252}\text{Cf}$  was estimated from

$$\omega \approx \frac{\nu}{E_T} \Big|_{\text{U}235} \quad \text{A.8)}$$

Values for  $\nu$  in aluminum and iron were obtained by interpolation of the results of Lindhard and Thomson.<sup>(15)</sup> Values for  $E_T$  were obtained by integration of the nuclear energy transfer functions for the MLF and MHF fragments of  $^{235}\text{U}$  in aluminum and iron. The results are given in Table I.

APPENDIX BMODEL TO ESTIMATE DISPLACEMENT DENSITY

The approximations described on p.6 were made to reduce the complexity of calculating the displaced atom density created by fission fragments emitted from a volumetric source. The first approximation (equal ranges in source and target) slightly overestimates the damage rate in aluminum, since the calculated ranges of the MHF and MLF fragments in Cf-oxide (taken as  $Cf_2O_3$ ) are about 20% less than those in aluminum. For an iron target, the damage rates calculated by this model are slightly underestimated. The second approximation greatly simplifies the integration of the product of fission fragment flux and nuclear energy loss rate.

The source geometry considered by this model is shown in Figure B.1. The fission fragment flux from a small volume  $dV$  in the source is simply  $n_f \cdot dV / 4\pi r^2$ , where  $n_f$  is the source density (f.f./ $cm^3$  sec). Using Equation 2, the displacement density produced at  $r$  by fission fragments emitted from  $dV$  can be expressed as

$$N(r)dV = \frac{n_f dV}{4\pi r^2} \cdot \frac{\omega S_n(r)}{2E_d} \quad B.1)$$

where  $dV = 2\pi r^2 \sin\theta \, dr d\theta$ . The other terms appearing in Equation B.1 were previously defined. Integrating over the effective source volume gives

$$N(x) = \frac{\omega E_T}{2E_d} \cdot 2\pi \int_{x/R_m}^1 d\mu \int_{x/4}^{R_m} r^2 dr \frac{n_f}{4\pi r^2} \cdot \frac{1}{\alpha\sqrt{\pi}} e^{-\left[\frac{R-r}{\alpha}\right]^2} \quad B.2)$$

where  $\mu = \cos\theta$ ,  $x$  is the depth of penetration of the fragments into the target (Figure B.1), and  $R_m$  is the maximum projected range of the MLF or MHF fragment. The upper limit on the second integral can be extended to infinity without changing the integral's value. Carrying out the integrations in Equation B.2 as far as possible in closed form gives

$$N(x) = \frac{\omega E_T}{8E_d} \left[ (1-x/R) + \alpha x \int_{\frac{R-R_m}{\alpha}}^{\frac{R-x}{\alpha}} \frac{\text{erf}(v)}{(R-\alpha v)^2} dv \right] \quad B.3)$$

where  $v = \frac{1}{\alpha}(R-x/\mu)$ .

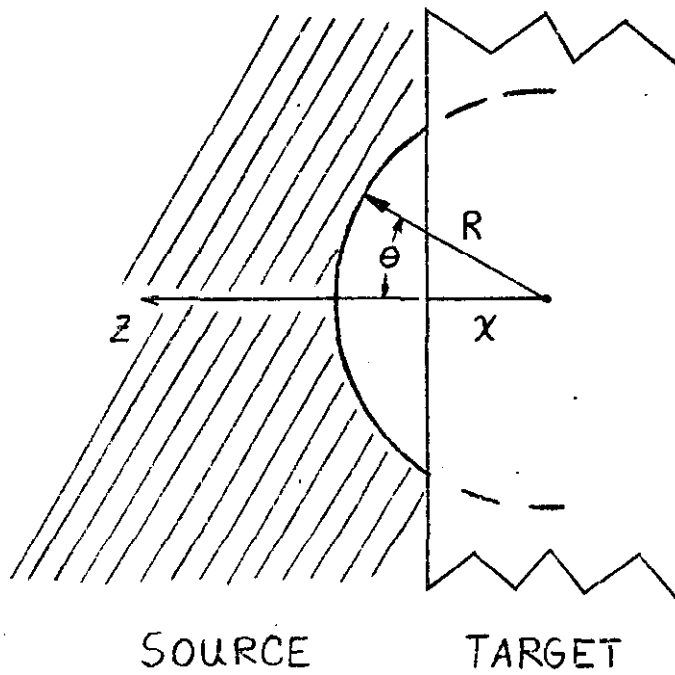


FIGURE B-1. Source-Target Geometry.

For all practical purposes, the maximum range can be set equal to the mean projected range plus twice the straggling parameter;  $R_m = R + 2\alpha$ . Making the substitution for  $R_m$ , Equation B.3 can be approximated by

$$N(x) \approx \frac{\eta f W E T}{4 E d} \left[ 1 - x \left( \frac{R}{R^2 - 4\alpha^2} \right) \right], \quad x < R - 2\alpha$$

or,

B.4)

$$N(x) \approx \frac{\eta f W E T}{4 E d} (1 - x/R)$$

for  $\alpha$  of the order of  $0.1R$  or less. Thus, the displacement density is expected to decrease almost linearly with the depth of penetration of the fission fragments.